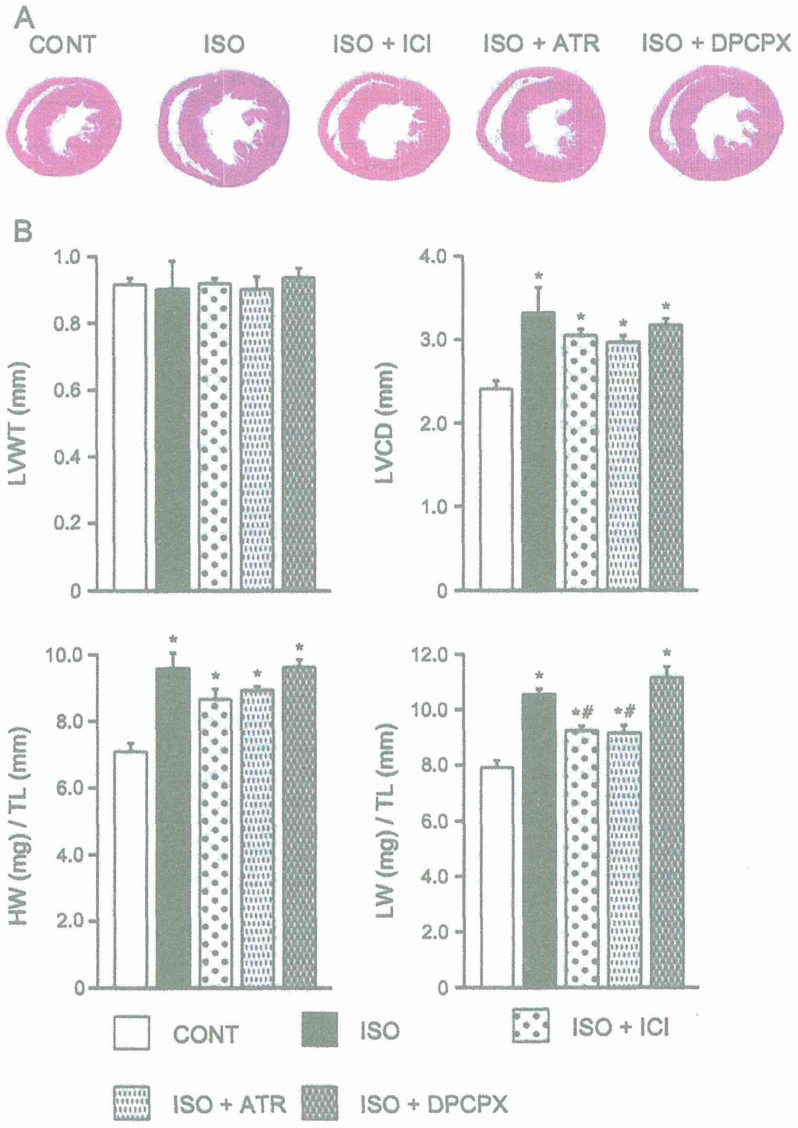

Fig. 1. Effect of antagonists on cardiac hypertrophy and failure in mice chronically treated with isoproterenol. (A) Low-magnification histological photographs of the ventricular cross section of hearts stained with hematoxylin–eosin. Original magnification 1.25×. (B) Left ventricular wall thickness (LVWT), left ventricular chamber diameter (LVCD), heart weight (HW)-to-tibial length (TL) ratio (HW/TL), and lung weight (LW)-to-tibial length ratio (LW/TL). Graphs show the mean ± S.E.M; n=6–10 for each group. CONT, control; ISO, isoproterenol; ICI, ICI118,551; ATR, atropine. *$P<0.05$ vs. CONT; #$P<0.05$ vs. ISO.

3. Results

3.1. Effect of inhibition of $G_{i/o}$ protein-coupled β_2-adrenergic, M_2-muscarinic and A_1-adenosine receptors on cardiac hypertrophy and failure in mice chronically treated with isoproterenol

We first examined whether inhibition of cardiac major $G_{i/o}$-coupled receptors (β_2-adrenergic, M_2-musucarinic, and A_1-adenosine receptors) with antagonists ameliorated the cardiac hypertrophy and failure of isoproterenol-treated mice. Namely, mice were treated with saline alone, isoproterenol alone, isoproterenol plus ICI118,551, isoproterenol plus atropine, or isoproterenol plus DPCPX. Mice treated with these drugs showed cardiac hypertrophy and dilation of ventricular chambers compared with those treated with saline (Fig. 1A). Although the left ventricular wall thickness (LVWT) was comparable in all groups, the left ventricular chamber diameter (LVCD) and HW/TL were significantly higher in mice treated with the drugs than those treated with saline (Fig. 1B), indicating that neither β_2-adrenergic, M_2-musucarinic, nor A_1-adenosine receptors contributed to isoproterenol-induced cardiac hypertrophy. LW/TL was also significantly higher in mice treated with the drugs than those treated with saline; however, LW/TL of mice treated with isoproterenol plus ICI118,551 or atropine was significantly lower than that of mice treated with isoproterenol alone (Fig. 1B), indicating that ICI118,551 and atropine ameliorated the congestive heart failure caused by isoproterenol.

Table 2 summarizes alterations in the HR and MBP during the treatment of mice with saline or the drugs. HR of mice treated with isoproterenol alone progressively decreased as compared with those treated with saline, which was not attenuated by ICI118,551, atropine or DPCPX, most likely as a consequence of downregulation of β_1-adrenergic receptors. MBP also progressively decreased in mice treated with the drugs as compared with those treated with saline; however, MBP of mice treated with isoproterenol plus ICI118,551 or atropine was significantly higher than that

of mice treated with isoproterenol alone, indicating that the effect of ICI118,551 and atropine on pulmonary edema was not due to their effect on the afterload of the heart.

M-mode ultrasound cardiogram showed that mice treated with isoproterenol alone exhibited increased end-diastolic and -systolic left ventricular diameters and decreased wall motion as compared with saline-treated mice as previously reported (Fig. 2A) (Horiuchi-Hirose et al., 2011). Mice treated with isoproterenol plus ICI118,551 or atropine exhibited smaller end-systolic left ventricular diameters and better wall motion than those treated with isoproterenol alone. These parameters of mice treated with isoproterenol plus DPCPX were comparable with those of mice treated with isoproterenol alone. Calculated fractional shortening (FS) of mice treated with isoproterenol plus ICI118,551 or atropine was significantly lower than that of mice treated with saline but significantly higher than that of mice treated with isoproterenol alone (Fig. 2B). FS was greatly decreased in mice treated with isoproterenol alone or isoproterenol plus DPCPX as compared with those treated with saline.

Hemodynamic assessment with catheterization showed that mice treated with the drugs exhibited significantly higher LVEDP and significantly smaller dP/dt_{max} and dP/dt_{min} than saline-treated mice (Fig. 3A–C) (Horiuchi-Hirose et al., 2011). However, mice treated with isoproterenol plus ICI118,551 or atropine exhibited significantly higher dP/dt_{max} and dP/dt_{min} and lower LVEDP than those treated with isoproterenol alone. These parameters of mice treated with isoproterenol plus DPCPX were comparable with those of mice treated with isoproterenol alone; therefore, β_2-adrenergic and M_2-muscarinic, but not A_1-adenosine receptors were involved in the cardiac dysfunction of isoproterenol-treated mice.

Table 2
Effect of chronic administration of receptor agonists and/or antagonists on the heart rate and mean systemic blood pressure of mice.

	CONT	ISO	ISO+ICI	ISO+ATR	ISO+DPCPX
Heat rate (beats/min)					
Before	665 ± 10	658 ± 12	654 ± 10	650 ± 10	653 ± 14
1 week later	673 ± 6	596 ± 4[a]	635 ± 13	613 ± 15[a]	589 ± 7[a]
2 weeks later	669 ± 7	551 ± 10[a]	569 ± 12[a]	583 ± 17[a]	544 ± 13[a]
3 weeks later	660 ± 11	546 ± 5[a]	560 ± 10[a]	559 ± 15[a]	534 ± 7[a]
Mean systemic blood pressure (mmHg)					
Before	81.2 ± 2.8	81.0 ± 2.1	80.7 ± 1.9	80.9 ± 1.6	83.7 ± 1.9
1 week later	80.6 ± 1.2	73.1 ± 1.3[a]	80.0 ± 1.5[b]	76.6 ± 1.1	72.7 ± 3.1[a]
2 weeks later	79.6 ± 0.5	66.8 ± 2.9[a]	75.3 ± 1.1[b]	76.4 ± 1.4[b]	68.8 ± 1.6[a]
3 weeks later	80.4 ± 0.9	64.7 ± 1.2[a]	76.4 ± 1.0[b]	71.8 ± 1.5[a,b]	68.3 ± 1.6[a]

Values are the mean ± S.E.M. $N=6$ for all groups. CONT, control; ISO, isoproterenol; ICI, ICI118,551; ATR, atropine.

[a] $P<0.05$ vs. CONT.

[b] $P<0.05$ vs. ISO.

3.2. Effect of inhibition of $G_{i/o}$ protein-coupled β_2-adrenergic, M_2-muscarinic and A_1-adenosin receptors on the L-type Ca^{2+} channel current density in mice chronically treated with isoproterenol

We previously demonstrated that chronic G protein-coupled receptor-mediated activation of $G_{i/o}$ decreased cardiac contractility at least partially by decreasing TT LTCC current density in isoproterenol-treated mice (Kashihara et al., 2012). We therefore assessed whether inhibition of β_2-adrenergic, M_2-muscarinic, and A_1-adenosine receptors normalized LTCC current density in myocytes of mice chronically treated with isoproterenol. Fig. 4A (solid lines) shows representative whole-cell LTCC currents of myocytes of each group of mice in response to depolarization to 0 mV from the prepulse of −50 mV. To separately assess SS and TT

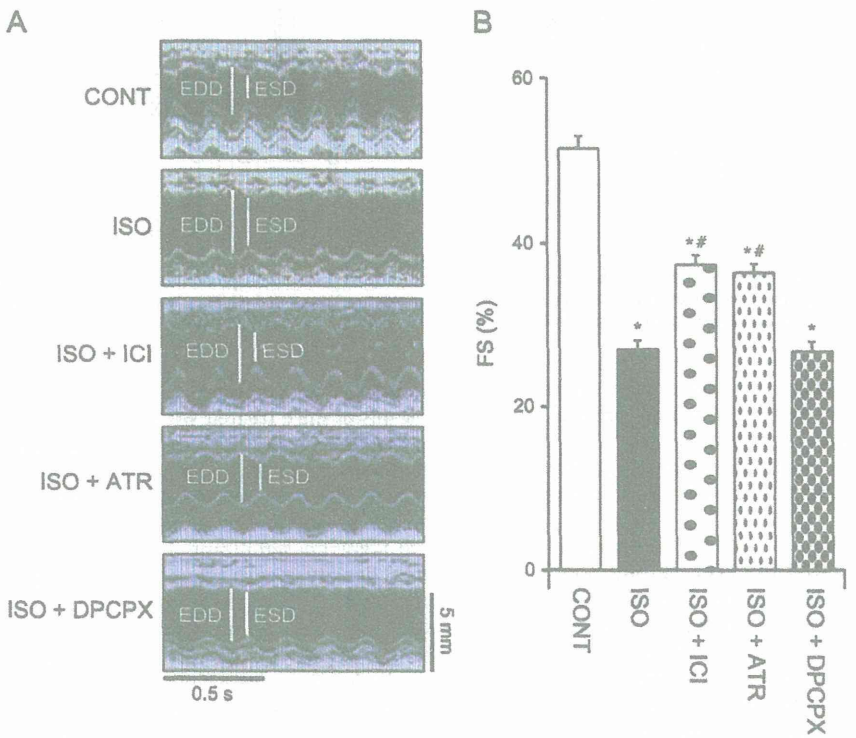

Fig. 2. Effect of antagonists on cardiac function assessed with ultrasound cardiogram in mice chronically treated with isoproterenol. (A) Representative M-mode ultrasound cardiogram traces. EDD, end-diastolic diameter; ESD, end-systolic diameter, (B) Fractional shortening (FS). Graphs show the mean ± S.E.M; $n=6$–10 for each group. CONT, control; ISO, isoproterenol; ICI, ICI118,551; ATR, atropine. *$P<0.05$ vs. CONT; #$P<0.05$ vs. ISO.

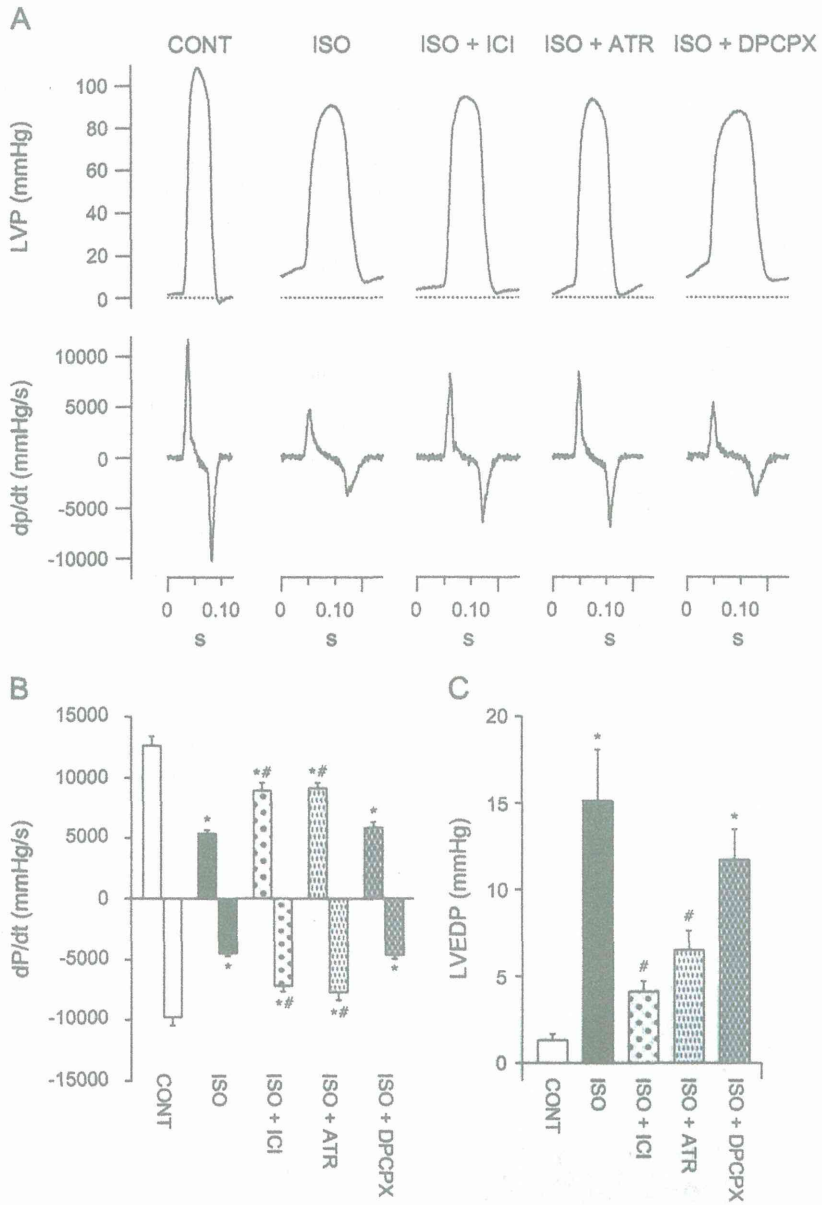

Fig. 3. Effect of antagonists on basal left-ventricular hemodynamic parameters of mice chronically treated with isoproterenol. (A) Representative traces of left ventricular pressure (LVP) and dP/dt (in mmHg/s). (B) The maximal and minimum rates of LVP development (dP/dt_{max} and dP/dt_{min}, respectively). (C) Left ventricular end-diastolic pressure (LVEDP). Graphs show the mean ± S.E.M; $n=5$ for each group. CONT, control; ISO, isoproterenol; ICI, ICI118,551; ATR, atropine. $^{*}P<0.05$ vs. CONT; $^{\#}P<0.05$ vs. ISO.

LTCC current densities, we measured LTCC currents in ventricular myocytes with detubulation, a procedure to acutely occlude TT in isolated ventricular myocytes (Horiuchi-Hirose et al., 2011; Kawai et al., 1999). As shown in Fig. 4A (broken lines), detubulation substantially reduced LTCC current amplitude in all groups of myocytes.

Fig. 4B shows the pooled data of the peak current–voltage relationships. Detubulation reduced the LTCC current amplitude by 62% in myocytes of saline-treated mice but by only 30% in those of isoproterenol-treated mice (Fig. 4A and B), indicating that TT LTCC currents were decreased in isoproterenol vs. saline-treated mice. On the other hand, detubulation reduced the LTCC current amplitude by 60% in myocytes of mice treated with isoproterenol plus ICI118,551; by 57%, isoproterenol plus atropine; and by 35%, isoproterenol plus DPCPX. Thus, inhibition of β_2-adrenergic and M_2-muscarinic, but not A_1-adenosine receptors may have attenuated the decreased TT LTCC current density found in myocytes of mice treated with isoproterenol.

From the peak LTCC current amplitude at 0 mV and the membrane capacitance of non-detubulated and detubulated myocytes (Table 1), we could assess the LTCC current density in SS and TT membrane compartments (Horiuchi-Hirose et al., 2011). There were no significant differences in whole-cell (WC) LTCC current density in each group of myocytes (Fig. 4C). In myocytes of saline-treated mice, there was ~5 times higher LTCC current density in the TT membrane than in the SS membrane (Horiuchi-Hirose et al., 2011). In myocytes of isoproterenol-treated mice, there were significantly higher SS and lower TT LTCC current densities than in myocytes of saline-treated mice. Notably, myocytes of mice treated with isoproterenol plus ICI118,551 or atropine but not DPCPX showed significantly lower SS and higher TT LTCC current densities than those of mice treated with

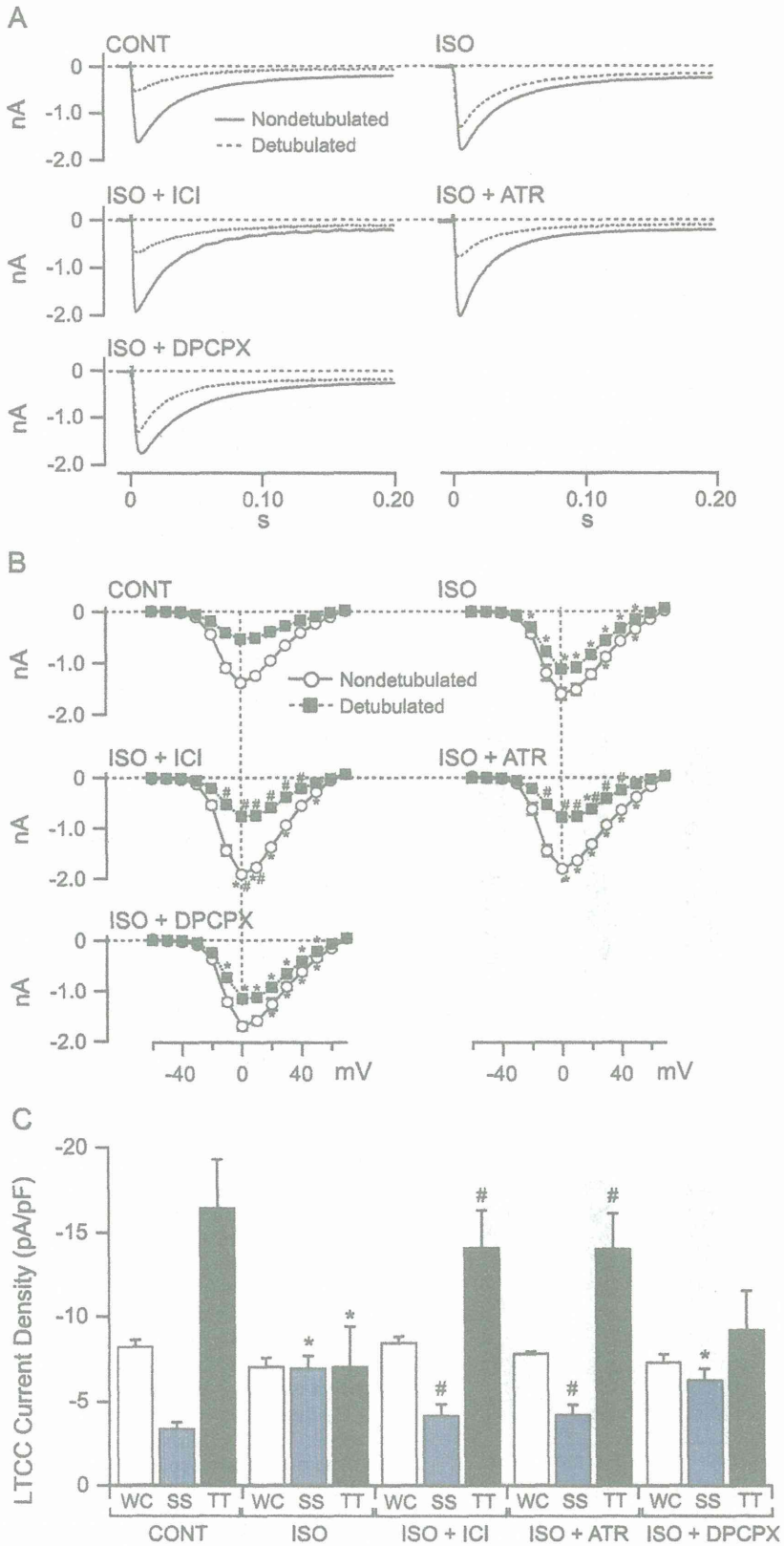

Fig. 4. Effect of antagonists on L-type Ca^{2+} channel current densities in whole cell, surface sarcolemmal, and t-tubular membranes in mice chronically treated with isoproterenol. (A) Representative L-type Ca^{2+} channel (LTCC) currents at 0 mV in CONT, ISO, ISO+ICI, ISO+ATR, and ISO+DPCPX myocytes with (broken lines) and without detubulation (solid lines). (B) Peak current–voltage relationships of LTCC currents in CONT, ISO, ISO+ICI, ISO+ATR, and ISO+DPCPX myocytes with (■) and without detubulation (○). (C) LTCC current density at 0 mV in whole-cell (WC), surface sarcolemmal (SS) and t-tubular (TT) membranes in CONT, ISO, ISO+ICI, ISO+ATR and ISO+DPCPX myocytes. Graphs show the mean ± S.E.M; n=6–8 for each group. CONT, control; ISO, isoproterenol; ICI, ICI118,551; ATR, atropine. *$P < 0.05$ vs. CONT; #$P < 0.05$ vs. ISO.

isoproterenol alone. The LTCC current densities in myocytes of mice treated with isoproterenol plus ICI118,551 and atropine were similar to those of myocytes of saline-treated mice; therefore, β_2-adrenergic and M_2-muscarinic receptors may have induced cardiac dysfunction in isoproterenol-treated mice at least partially by decreasing TT LTCC activity.

3.3. Effect of inhibition of protein phosphatases on the L-type Ca^{2+} channel current density in each group of mice

We previously reported that in isoproterenol-treated mice, SS LTCC current density is increased due to $G_{i/o}$-mediated suppression of PP1 whereas TT LTCC current density is decreased due to $G_{i/o}$-mediated activation of PP2A (Horiuchi-Hirose et al., 2011; Kashihara et al., 2012). Thus, we finally examined whether ICI118,551 and atropine normalized SS and TT LTCC current densities by ameliorating the abnormal PP activities. Fig. 5A shows the WC, SS and TT LTCC current densities in each group of mice in the presence of okadaic acid (OA) (1 μM), a PP1 and PP2A inhibitor, where the difference in SS and TT LTCC densities among groups was abolished. This indicates that isoproterenol caused the abnormal LTCC densities whereas ICI118,551 and atropine, but not DPCPX normalized the LTCC densities by modifying PP1 and/or 2A. Fig. 5B shows the results in the presence of fostriecin (1 μM), a selective PP2A inhibitor. Under this condition, the difference in TT but not SS LTCC densities among groups was abolished, indicating that isoproterenol decreased the TT LTCC density by stimulating PP2A whereas ICI118,551 and atropine, but not DPCPX increased the TT LTCC density by inhibiting PP2A. Together with Fig. 5A and B also indicates that isoproterenol increased the SS LTCC density by inhibiting PP1 whereas ICI118,551 and atropine, but not DPCPX decreased the SS LTCC density by activating PP1.

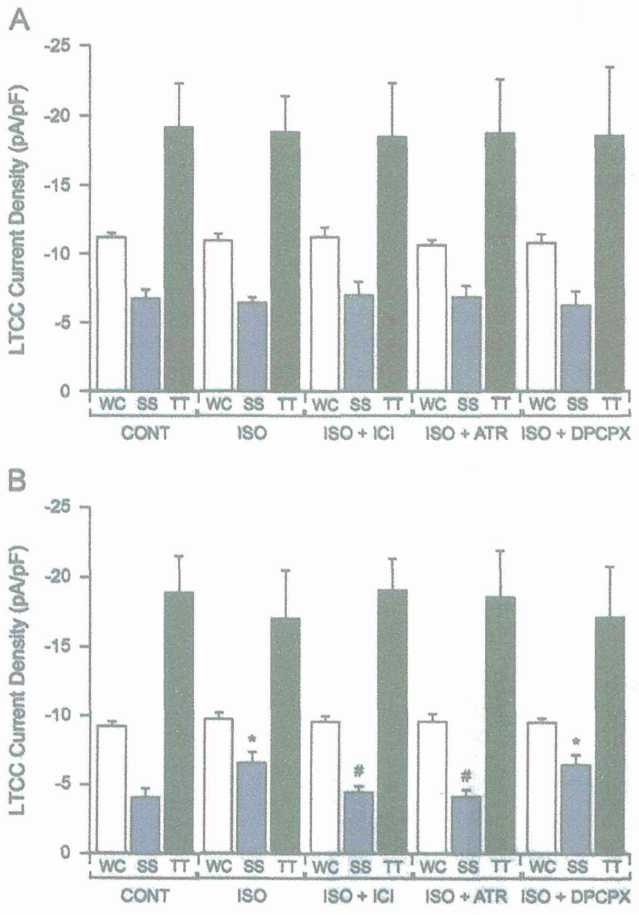

Fig. 5. Effect of a protein phosphatase 1 and 2A inhibitor, okadaic acid, and a selective protein phosphatase 2A inhibitor, fostriecin on L-type Ca^{2+} channel (LTCC) current densities in whole-cell (WC), surface sarcolemmal (SS), and t-tubular membranes (TT). (A and B) LTCC current density at 0 mV in WC, SS, and TT in CONT, ISO, ISO+ICI, ISO+ATR, and ISO+DPCPX myocytes in the presence of okadaic acid (1 μM) (A) or fostriecin (1 μM) (B). Graphs show the mean ± S.E.M; n=5–6 for each group. CONT, control; ISO, isoproterenol; ICI, ICI118,551; ATR, atropine. *P < 0.05 vs. CONT; #P < 0.05 vs. ISO.

4. Discussion

In heart failure, chronic and excessive β-adrenergic receptor stimulation causes remodeling of the myocardium and aggravates cardiac function (Osadchii, 2007; Rockman et al., 2002). This concept is the theoretical basis for the treatment of heart failure with β-adrenergic antagonists. In experiments, transgenic overexpression of β_1-adrenergic receptors in the murine heart causes dilated cardiomyopathy (Engelhardt et al., 1999). We also found that metoprolol, a selective β_1-adrenergic antagonist, almost completely prevented cardiac hypertrophy and failure of isoproterenol-treated mice (data not shown), indicating that excessive stimulation of β_1-adrenergic receptors is the primary cause of myocardial remodeling in isoproterenol-treated mice (Osadchii, 2007; Xiao et al., 2006). However, we also previously found that chronic administration of pertussis toxin significantly improved the cardiac function of isoproterenol-treated mice, indicating that $G_{i/o}$ chronically activated by some G protein-coupled receptors participate in the cardiac dysfunction of isoproterenol-treated mice (Kashihara et al., 2012). Consistent with this observation, it is reported that the increased activity of $G_{i/o}$ suppresses cardiac function in heart failure (El-Armouche et al., 2003). In the present study, we sought to identify $G_{i/o}$ protein-coupled receptors contributing to the cardiac dysfunction of isoproterenol-treated mice. Compared with mice treated with isoproterenol alone, mice treated with isoproterenol plus ICI118,551 or atropine, but not DPCPX showed significantly lower LW/TL (Fig. 1B) and better hemodynamic parameters (i.e. higher FS (Fig. 2B), lower LVEDP, and higher dP/dt_{max} and dP/dt_{min} (Fig. 3B and C)). In addition, myocytes of mice treated with isoproterenol plus ICI118,551 or atropine, but not DPCPX exhibited significantly higher TT and lower SS LTCC current densities than those of mice treated with isoproterenol alone (Fig. 4C) due to normalization of PP activities (Fig. 5). Thus, chronic activation of β_2-adrenergic and M_2-muscarinic, but not A_1-adenosine receptors may cause cardiac dysfunction at least partially by decreasing basal TT LTCC activity in isoproterenol-treated mice. It is, however, necessary to confirm the present finding in more clinically relevant models of heart failure, such as those induced by pressure/volume overload or myocardial infarction, in future.

It is uncertain whether $G_{i/o}$ was activated by ligand-independent (i.e. basal) or -dependent activity of β_2-adrenergic and M_2-muscarinic receptors in isoproterenol-treated mice because ICI118,551 and atropine exert inverse agonism under some conditions (Nelson et al., 2006; Zhou et al., 1999). In animal models of heart failure and patients with idiopathic dilated cardiomyopathy, the expression level of M_2-muscaric receptors is increased (Le Guludec et al., 1997; Vatner et al., 1996). It is also known that β_2-adrenergic receptors become more efficiently coupled with $G_{i/o}$ in a failing than in a normal heart (Daaka et al., 1997; Liu et al., 2009; Paur et al., 2012). These changes of M_2-muscarinic and β_2-adrenergic receptors chronically increase $G_{i/o}$ activity independently of their ligands. Indeed, we found that abnormal LTCC activities persisted at least for several hours in isolated myocytes of isoproterenol-treated mice in the absence of any G protein-coupled receptor agonists (Horiuchi-Hirose et al., 2011; Kashihara et al., 2012). On the other hand, it is

also possible that β_2-adrenergic and M_2-muscarinic receptors were activated by their ligands in vivo. Although isoproterenol administrated to mice must have stimulated β_2-adrenergic receptors, adrenaline secreted from the adrenal medulla would also have activated β_2-adrenergic receptors because its plasma concentration increases in heart failure (Kaye et al., 1995; Paur et al., 2012). It is somewhat surprising that acetylcholine acting on M_2-muscarinic receptors worsens heart failure because many experimental studies have demonstrated that vagal stimulation has beneficial effects on heart failure (Kishi, 2012). Recently, Kanazawa et al. (2010) reported that the cardiac sympathetic nervous system exhibits cholinergic transdifferentiation in heart failure. Thus, one possibility is that such aberrant acetylcholine might cause deteriorating effects on failing cardiac myocytes. Probably, both ligand-independent and -dependent activities of β_2-adrenergic and M_2-muscarinic receptors cause abnormal LTCC activities and cardiac function under excessive β_1-adrenergic stimulation in heart failure.

$G_{i/o}$ inhibits adenylyl cyclase (Sunahara et al., 1996). Thus, ICI118,551 and atropine might have improved cardiac function by increasing cAMP concentration in myocytes; however, neither mice treated with isoproterenol plus ICI118,551 nor atropine exhibited significantly higher HR than mice treated with isoproterenol alone (Table 2), contrary to this speculation. Moreover, we previously found that a selective protein kinase A inhibitor, H-89 did not affect SS or TT LTCC activity in ventricular myocytes of mice chronically treated with isoproterenol plus pertussis toxin, indicating that the chronic inhibition of $G_{i/o}$ did not significantly increase cAMP concentration in cardiac myocytes (Kashihara et al., 2012). We propose that ICI118,551 and atropine increased cardiac function of isoproterenol-treated mice by normalizing the abnormal effects of PPs on basal LTCC activity independently of protein kinase A (Fig. 5). ICI118,551 and atropine each separately substantially reversed the effect of isoproterenol on many parameters measured in this study: i.e. these drug effects were not additive. This was probably because β_2-adrenergic and M_2-muscarinic receptors shared $G_{i/o}$ proteins and PPs as a common pathway. Although Liu and Hofmann (2003) reported that activation of A_1-adenosine receptors lead to PP2A-induced dephosphorylation of phospholamban and troponin T in cardiac myocytes, we did not see significant effects of DPCPX on LTCC activity. PP2A has many different subunit compositions and, depending on the composition, different subcellular localization and different regulation (Janssens and Goris, 2001). Thus, we speculate that PP2A associated with LTCC may not be regulated by A_1-adenosine receptors in cardiac myocytes.

5. Conclusion

To summarize, for the first time, we found that chronic activation of $G_{i/o}$ through β_2-adrenergic and M_2-muscarinic, but not A_1-adenosine receptors compromises cardiac contractility at least partially by altering basal TT LTCC activity in heart failure. Thus, selective antagonists of β_2-adrenergic and M_2-muscarinic receptors may be useful in the treatment of chronic heart failure with excessive β-adrenergic stimulation; however, it is known that increased $G_{i/o}$ activity is not only harmful but also protective of a failing heart because it prevents excessive G_s/cAMP/protein kinase A stimulation. Therefore, it would be desirous to use these antagonists in heart failure in conjunction with β_1-adrenergic blockers that suppress G_s activity.

Acknowledgments

We are grateful to Ms. Reiko Sakai for secretarial assistance. This work was supported by research grants to M.Y. (21590275) and T.K. (24790210) from the Japan Society for the Promotion of Sciences (JSPS).

References

Bers, D.M., 2008. Heart failure. In: Bers, D.M. (Ed.), Excitation–Contraction Coupling and Cardiac Contractile Force. Springer, Dordrecht, The Netherlands, pp. 316–323.

Daaka, Y., Luttrell, L.M., Lefkowitz, R.J., 1997. Switching of the coupling of the beta$_2$-adrenergic receptor to different G proteins by protein kinase A. Nature 390, 88–91.

El-Armouche, A., Zolk, O., Rau, T., Eschenhagen, T., 2003. Inhibitory G-proteins and their role in desensitization of the adenylyl cyclase pathway in heart failure. Cardiovasc. Res. 60, 478–487.

Engelhardt, S., Hein, L., Wiesmann, F., Lohse, M.J., 1999. Progressive hypertrophy and heart failure in beta1-adrenergic receptor transgenic mice. Proc. Natl. Acad. Sci. USA 96, 7059–7064.

Go, A.S., Mozaffarian, D., Roger, V.L., Benjamin, E.J., Berry, J.D., Borden, W.B., Bravata, D.M., Dai, S., Ford, E.S., Fox, C.S., Franco, S., Fullerton, H.J., Gillespie, C., Hailpern, S.M., Heit, J.A., Howard, V.J., Huffman, M.D., Kissela, B.M., Kittner, S.J., Lackland, D.T., Lichtman, J.H., Lisabeth, L.D., Magid, D., Marcus, G.M., Marelli, A., Matchar, D.B., McGuire, D.K., Mohler, E.R., Moy, C.S., Mussolino, M.E., Nichol, G., Paynter, N.P., Schreiner, P.J., Sorlie, P.D., Stein, J., Turan, T.N., Virani, S.S., Wong, N.D., Woo, D., Turner, M.B., 2013. Heart disease and stroke statistics—2013 update: a report from the American Heart Association. Circulation 127, e6–e245.

Herzig, S., Meier, A., Pfeiffer, M., Neumann, J., 1995. Stimulation of protein phosphatases as a mechanism of the muscarinic-receptor-mediated inhibition of cardiac L-type Ca^{2+} channels. Pflugers Arch. 429, 531–538.

Horiuchi-Hirose, M., Kashihara, T., Nakada, T., Kurebayashi, N., Shimojo, H., Shibazaki, T., Sheng, X., Yano, S., Hirose, M., Hongo, M., Sakurai, T., Moriizumi, T., Ueda, H., Yamada, M., 2011. Decrease in the density of t-tubular L-type Ca^{2+} channel currents in failing ventricular myocytes. Am. J. Physiol. Heart Circ. Physiol. 300, H978–H988.

Janssens, V., Goris, J., 2001. Protein phosphatase 2A: a highly regulated family of serine/threonine phosphatases implicated in cell growth and signalling. Biochem. J. 353, 417–439.

Jumrussirikul, P., Dinerman, J., Dawson, T.M., Dawson, V.L., Ekelund, U., Georgakopoulos, D., Schramm, L.P., Calkins, H., Snyder, S.H., Hare, J.M., Berger, R.D., 1998. Interaction between neuronal nitric oxide synthase and inhibitory G protein activity in heart rate regulation in conscious mice. J. Clin. Invest. 102, 1279–1285.

Kanazawa, H., Ieda, M., Kimura, K., Arai, T., Kawaguchi-Manabe, H., Matsuhashi, T., Endo, J., Sano, M., Kawakami, T., Kimura, T., Monkawa, T., Hayashi, M., Iwanami, A., Okano, H., Okada, Y., Ishibashi-Ueda, H., Ogawa, S., Fukuda, K., 2010. Heart failure causes cholinergic transdifferentiation of cardiac sympathetic nerves via gp130-signaling cytokines in rodents. J. Clin. Invest. 120, 408–421.

Kashihara, T., Nakada, T., Gomi, S., Hirose, M., Yamada, M., 2013. The molecular mechanism by which chronic and excessive β1 adrenergic stimulation remodels ventricular excitation contraction coupling. J. Physiol. Sci. 63, S94.

Kashihara, T., Nakada, T., Shimojo, H., Horiuchi-Hirose, M., Gomi, S., Shibazaki, T., Sheng, X., Hirose, M., Hongo, M., Yamada, M., 2012. Chronic receptor-mediated activation of $G_{i/o}$ proteins alters basal t-tubular and sarcolemmal L-type Ca^{2+} channel activity through phosphatases in heart failure. Am. J. Physiol. Heart Circ. Physiol. 302, H1645–H1654.

Kawai, M., Hussain, M., Orchard, C.H., 1999. Excitation–contraction coupling in rat ventricular myocytes after formamide-induced detubulation. Am. J. Physiol. 277, H603–H609.

Kaye, D.M., Lefkovits, J., Cox, H., Lambert, G., Jennings, G., Turner, A., Esler, M.D., 1995. Regional epinephrine kinetics in human heart failure: evidence for extra-adrenal, nonneural release. Am. J. Physiol. 269, H182–H188.

Ke, Y., Wang, L., Pyle, W.G., de Tombe, P.P., Solaro, R.J., 2004. Intracellular localization and functional effects of P21-activated kinase-1 (Pak1) in cardiac myocytes. Circ. Res. 94, 194–200.

Kishi, T., 2012. Heart failure as an autonomic nervous system dysfunction. J. Cardiol. 59, 117–122.

Koeppen, M., Eckle, T., Eltzschig, H.K., 2009. Selective deletion of the A_1 adenosine receptor abolishes heart-rate slowing effects of intravascular adenosine in vivo. PloS One 4, e6784.

Le Guludec, D., Cohen-Solal, A., Delforge, J., Delahaye, N., Syrota, A., Merlet, P., 1997. Increased myocardial muscarinic receptor density in idiopathic dilated cardiomyopathy: an in vivo PET study. Circulation 96, 3416–3422.

Liu, Q., Hofmann, P.A., 2003. Modulation of protein phosphatase 2a by adenosine A_1 receptors in cardiomyocytes: role for p38 MAPK. Am. J. Physiol. Heart. Circ. Physiol. 285, H97–H103.

Liu, R., Ramani, B., Soto, D., De Arcangelis, V., Xiang, Y., 2009. Agonist dose-dependent phosphorylation by protein kinase A and G protein-coupled receptor kinase regulates beta2 adrenoceptor coupling to G_i proteins in cardiomyocytes. J. Biol. Chem. 284, 32279–32287.

Mann, D.L., 2008. Pathophysiology of heart failure. In: Libby, P., Bonow, R.O., Mann, D.L., Zipes, D.P., Braunwald, E. (Eds.), Heart Diseases. Saunders Elsevier, Philadelphia, pp. 541–560.

McDonald, T.F., Pelzer, S., Trautwein, W., Pelzer, D.J., 1994. Regulation and modulation of calcium channels in cardiac, skeletal, and smooth muscle cells. Physiol. Rev. 74, 365–507.

Mukherjee, R., Spinale, F.G., 1998. L-type calcium channel abundance and function with cardiac hypertrophy and failure: a review. J. Mol. Cell Cardiol. 30, 1899–1916.

Nelson, C.P., Nahorski, S.R., Challiss, R.A., 2006. Constitutive activity and inverse agonism at the M_2 muscarinic acetylcholine receptor. J. Pharmacol. Exp. Ther. 316, 279–288.

Osadchii, O.E., 2007. Cardiac hypertrophy induced by sustained beta-adrenoreceptor activation: pathophysiological aspects. Heart Fail. Rev. 12, 66–86.

Paur, H., Wright, P.T., Sikkel, M.B., Tranter, M.H., Mansfield, C., O'Gara, P., Stuckey, D. J., Nikolaev, V.O., Diakonov, I., Pannell, L., Gong, H., Sun, H., Peters, N.S., Petrou, M., Zheng, Z., Gorelik, J., Lyon, A.R., Harding, S.E., 2012. High levels of circulating epinephrine trigger apical cardiodepression in a $beta_2$-adrenergic receptor/G_i-dependent manner: a new model of Takotsubo cardiomyopathy. Circulation 126, 697–706.

Rockman, H.A., Koch, W.J., Lefkowitz, R.J., 2002. Seven-transmembrane-spanning receptors and heart function. Nature 415, 206–212.

Sunahara, R.K., Dessauer, C.W., Gilman, A.G., 1996. Complexity and diversity of mammalian adenylyl cyclases. Annu. Rev. Pharmacol. Toxicol. 36, 461–480.

Uechi, M., Asai, K., Osaka, M., Smith, A., Sato, N., Wagner, T.E., Ishikawa, Y., Hayakawa, H., Vatner, D.E., Shannon, R.P., Homcy, C.J., Vatner, S.F., 1998. Depressed heart rate variability and arterial baroreflex in conscious transgenic mice with overexpression of cardiac $G_{s\alpha}$. Circ. Res. 82, 416–423.

Vatner, D.E., Sato, N., Galper, J.B., Vatner, S.F., 1996. Physiological and biochemical evidence for coordinate increases in muscarinic receptors and G_i during pacing-induced heart failure. Circulation 94, 102–107.

Xiao, R.P., Zhu, W., Zheng, M., Cao, C., Zhang, Y., Lakatta, E.G., Han, Q., 2006. Subtype-specific $alpha_1$- and beta-adrenoceptor signaling in the heart. Trends Pharmacol. Sci. 27, 330–337.

Yamada, M., Ohta, K., Niwa, A., Tsujino, N., Nakada, T., Hirose, M., 2008. Contribution of L-type Ca^{2+} channels to early afterdepolarizations induced by I_{Kr} and I_{Ks} channel suppression in guinea pig ventricular myocytes. J. Membr. Biol. 222, 151–166.

Zhou, Y.Y., Cheng, H., Song, L.S., Wang, D., Lakatta, E.G., Xiao, R.P., 1999. Spontaneous $beta_2$-adrenergic signaling fails to modulate L-type Ca^{2+} current in mouse ventricular myocytes. Mol. Pharmacol. 56, 485–493.

Zhu, M., Gach, A.A., Liu, G., Xu, X., Lim, C.C., Zhang, J.X., Mao, L., Chuprun, K., Koch, W.J., Liao, R., Koren, G., Blaxall, B.C., Mende, U., 2008. Enhanced calcium cycling and contractile function in transgenic hearts expressing constitutively active $G_{\alpha o}{}^*$ protein. Am. J. Physiol. Heart Circ. Physiol. 294, H1335–H1347.

Cardiovascular Research (2013) 99, 461–470
doi:10.1093/cvr/cvt122

Deficiency of senescence marker protein 30 exacerbates angiotensin II-induced cardiac remodelling

Tomofumi Misaka[1], Satoshi Suzuki[1], Makiko Miyata[1], Atsushi Kobayashi[1], Tetsuro Shishido[2], Akihito Ishigami[3], Shu-ichi Saitoh[1], Masamichi Hirose[4], Isao Kubota[2], and Yasuchika Takeishi[1]*

[1]Department of Cardiology and Hematology, Fukushima Medical University, 1 Hikarigaoka, Fukushima 960-1295, Japan; [2]First Department of Internal Medicine, Yamagata University School of Medicine, Yamagata, Japan; [3]Molecular Regulation of Aging, Tokyo Metropolitan Institute of Gerontology, Tokyo, Japan; and [4]Department of Molecular and Cellular Pharmacology, Iwate Medical University School of Pharmaceutical Science, Iwate, Japan

Received 17 December 2012; revised 11 May 2013; accepted 15 May 2013; online publish-ahead-of-print 30 May 2013

Time for primary review: 37 days

Aims Ageing is an important risk factor of cardiovascular diseases including heart failure. Senescence marker protein 30 (SMP30), which was originally identified as an important ageing marker protein, is assumed to act as a novel anti-ageing factor in various organs. However, the role of SMP30 in the heart has not been previously explored. In this study, our aim was to elucidate the functional role of SMP30 on cardiac remodelling.

Methods and results SMP30 knockout (KO) mice and wild-type (WT) mice were subjected to continuous angiotensin II (Ang II) infusion. After 14 days, the extent of cardiac hypertrophy and myocardial fibrosis was significantly higher in SMP30-KO mice than in WT mice. Echocardiography revealed that SMP30-KO mice had more severely depressed systolic and diastolic function with left ventricular dilatation compared with WT mice. Generation of reactive oxygen species related with activation of nicotinamide adenine dinucleotide phosphate-oxidase was greater in SMP30-KO mice than in WT mice. The number of deoxynucleotidyl transferase-mediated dUTP nick end-labelling positive nuclei was markedly increased in SMP30-KO mice with activation of caspase-3, increases in the Bax to Bcl-2 ratio and phosphorylation of c-Jun N-terminal kinase compared with WT mice. Furthermore, the number of senescence-associated β-galactosidase-positive cells was significantly increased via up-regulation of p21 gene expression in SMP30-KO mice compared with WT mice.

Conclusion This study demonstrated the first evidence that deficiency of SMP30 exacerbates Ang II-induced cardiac hypertrophy, dysfunction, and remodelling, suggesting that SMP30 has a cardio-protective role in cardiac remodelling with anti-oxidative and anti-apoptotic effects in response to Ang II.

Keywords Senescence marker protein 30 (SMP30) • Ageing • Remodelling • Oxidative stress • Apoptosis

1. Introduction

The prevalence and mortality rate of heart failure dramatically increase in older people, and ageing is one of the risk factors for cardiovascular events.[1] With ageing, the heart shows changes in cardiac structure and function. Age-associated cardiac remodelling includes an enlargement of cardiomyocyte size, loss of myocytes due to apoptosis or necrosis, and increase of matrix connective tissue. These age-associated cardiac changes seem to be relevant to the steep increases in left ventricular hypertrophy, diastolic dysfunction, and subsequent heart failure.[2]

Oxidative stress is considered to be an important factor in controlling heart ageing.[3] It is well known that the renin–angiotensin system (RAS) is a central component of the physiological and pathological responses of the cardiovascular system. Activation of RAS is a significant driver of oxidative stress and is involved in age-related cardiac remodelling. Angiotensin II (Ang II), the primary effector molecule of RAS, contributes not only to vasoconstriction and hypertension, but also to cardiac hypertrophy, remodelling, and heart failure. Therefore, Ang II signalling appears to play a critical role in heart ageing.

* Corresponding author. Tel: +81 245471190; fax: +81 245481821. Email: takeishi@fmu.ac.jp

Senescence marker protein 30 (SMP30), a 34-kDa protein, was originally identified as a novel ageing marker protein in rat liver, whose expression decreases androgen-independently with age.[4] SMP30 transcripts are detected in almost all organs, and the SMP30 gene is highly conserved among numerous animal species including humans.[5] Intracellular localization of SMP30 is in the cytoplasm and perinuclear regions, and SMP30 exists in multiple forms under physiological conditions.[6] It has been demonstrated that SMP30 plays multifunctional roles as Ca^{2+} regulator (named as regucalcin),[7] anti-oxidant,[8] and enzymatic ability to hydrolyze di-isopropyl phosphorofluoridate.[9] Recently, SMP30 has been determined as gluconolactonase, which is involved in ascorbic acid (vitamin C) biosynthesis in mammals, whereas human beings are unable to synthesize vitamin C *in vivo* because of mutations in L-gulonolactone oxidase.[10]

SMP30-knockout (KO) mice have been generated[11] and showed a shorter life span than that of the wild-type (WT) mice on a vitamin C-deficient diet.[12] Using SMP30-KO mice, recent reports have demonstrated that SMP30 functions to protect cells from apoptosis in the liver[11] and that SMP30 has protective effects against age-associated oxidative stress in the brain[13] and lungs.[14] Furthermore, SMP30-KO mice have shown accelerated senescence in the kidney[15] and the worsening of glucose tolerance.[16] Taken together, SMP30 is assumed to behave as an anti-ageing factor. However, the role of SMP30 in the heart has not been previously explored.

We hypothesized that SMP30 has cardio-protective functions from harmful stimuli with anti-oxidative and anti-apoptotic effects. To test the hypothesis, we used SMP30-KO mice to examine the effects of SMP30 on Ang II-induced cardiac hypertrophy and remodelling *in vivo*.

2. Methods

For additional detailed methods, please see Supplementary material online..

2.1 Animal protocol

SMP30-KO (C57BL/6 background) mice were established as previously reported.[11] Drinking water containing vitamin C (1.5 g/L) was provided for the SMP30-KO mice to avoid vitamin C deficiency due to their inability to synthesize vitamin C *in vivo*.[10] After anaesthetizing the mice by i.p. injection of pentobarbital (50 mg/kg body weight), an osmotic minipump (ALZET micro-osmotic pump MODEL 1002, DURECT Co., Cupertino, CA, USA) was subcutaneously implanted, and Ang II (800 ng/kg/min) was continuously infused for 14 days.[17,18] Controls were administered saline. The investigations conformed to the *Guide for the Care and Use of Laboratory Animals* published by the US National Institutes of Health (NIH publication, 8th Edition, 2011). Our research protocol was approved by the institutional review board, and all animal experiments were conducted in accordance with the guidelines of Fukushima Medical University Animal Research Committee.

2.2 Measurement of vitamin C

Total vitamin C levels in the heart were measured by the dinitrophenylhydrazine method according to the manufacturer's protocol (SHIMA Laboratories Co. Ltd., Tokyo, Japan).[19]

2.3 Measurements of blood pressure and heart rate

Mice were implanted with a radiotelemetry probe (TA11PA-C22, Data Sciences International, St Paul, MN, USA) under i.p. anaesthesia by pentobarbital (50 mg/kg body weight) as described previously.[20] After a recovery phase of 10 days, basal arterial pressure and heart rate (HR) were started to recorded. After the measurement of control, Ang II was subcutaneously infused via an osmotic minipump, and the data were recorded.

2.4 Echocardiography

Transthoracic echocardiography was performed using Vevo 2100 High-Resolution *In Vivo* Imaging System (Visual Sonics, Inc., Toronto, Canada) with a high-resolution 40-MHz imaging transducer as previous reports described.[21,22] Mice were lightly anaesthetized by titrating isoflurane (0.5–1.5%) to achieve an HR of ~400 b.p.m., and all the measurements were obtained from three cardiac cycles.

2.5 Cardiac catheterization

The cardiac catheterization was performed as described previously.[23] Briefly, mice were anaesthetized by i.p. injection of 2,2,2-tribromo-ethanol (250 mg/kg body weight), the right carotid artery was cannulated with the micropressure transducer (samba preclin 420 LP, Samba Sensors AB, Gothenburg, Sweden) into the left ventricle. Adequacy of anaesthesia was monitored by HR, aortic blood pressure, and respiratory rate as well as the absence of reactions of painful stimuli. The data were measured using the Labscribe 2 software (iWorx Systems, Inc., Dover, NH, USA).

2.6 Histopathological analysis

After continuous infusion of Ang II or saline for 14 days, mice were sacrificed by cervical dislocation and hearts were rapidly excised. The paraffin-embedded heart sections were stained with haematoxylin and eosin or Elastica-Masson. The cross-sectional area of cardiomyocyte and fibrosis fraction was measured using the NIH ImageJ software (National Institutes of Health, Bethesda, MD, USA) and Adobe Photoshop CS2 (Adobe, San Jose, CA, USA).[24]

In immunohistochemical analysis, the paraffin-embedded sections were incubated with anti-SMP30 antibody (SHIMA Laboratories Co. Ltd., Tokyo, Japan) with a dilution of 1:200 or negative control (normal serum). The sections were stained with horseradish peroxidase-conjugated secondary antibody (Histofine Simple Stain Mouse MAX PO (R), Nichirei Biosciences, Inc., Tokyo, Japan) and diaminobenzidine etrahydrochloride, and counterstained with haematoxylin.

2.7 Assessment of reactive oxygen species generation

The fresh-frozen heart sections were incubated with 10 μmol/L dihydroethidium (DHE, Sigma-Aldrich Co., St Louis, MO, USA).[25,26] The fluorescent images were acquired using fluorescence microscope (Olympus IX71, OLYMPUS Optical Co., Tokyo, Japan) and the mean DHE fluorescence intensity of cardiomyocytes was quantitated with the NIH imageJ software.[26] In addition, 10 mmol/L apocynin, a nicotinamide adenine dinucleotide phosphate (NADPH) oxidase inhibitor, was provided in drinking water with Ang II continuous infusion, and reactive oxygen species (ROS) generation was evaluated by DHE staining.[27]

2.8 Western blotting

Total protein was extracted from the snap-frozen left ventricle using Cell Lysis Buffer (Cell Signaling Technology, Inc., Beverly, MA, USA) with Protease Inhibitor Cocktail (BD Biosciences, San Jose, CA, USA) as previous reports described.[24] The primary antibodies were as follows: anti-SMP30, anti-67^{phox}, anti-Bax, anti-Bcl-2, anti-phospho-stress-activated protein kinase/c-Jun N-terminal kinase (SAPK/JNK, Thr183/Tyr185), anti-SAPK/JNK (Cell Signaling Technology, Inc.), anti-activated-caspase-3 (Bioworld Technology, Inc., Minneapolis, MN, USA), and mouse anti-β-actin (Santa Cruz Biotechnology, Inc.). The signals from immunoreactive bands were visualized by an Amersham ECL system (Amersham Pharmacia Biotech UK Ltd., Buckinghamshire, UK) and quantified using densitometric analysis.

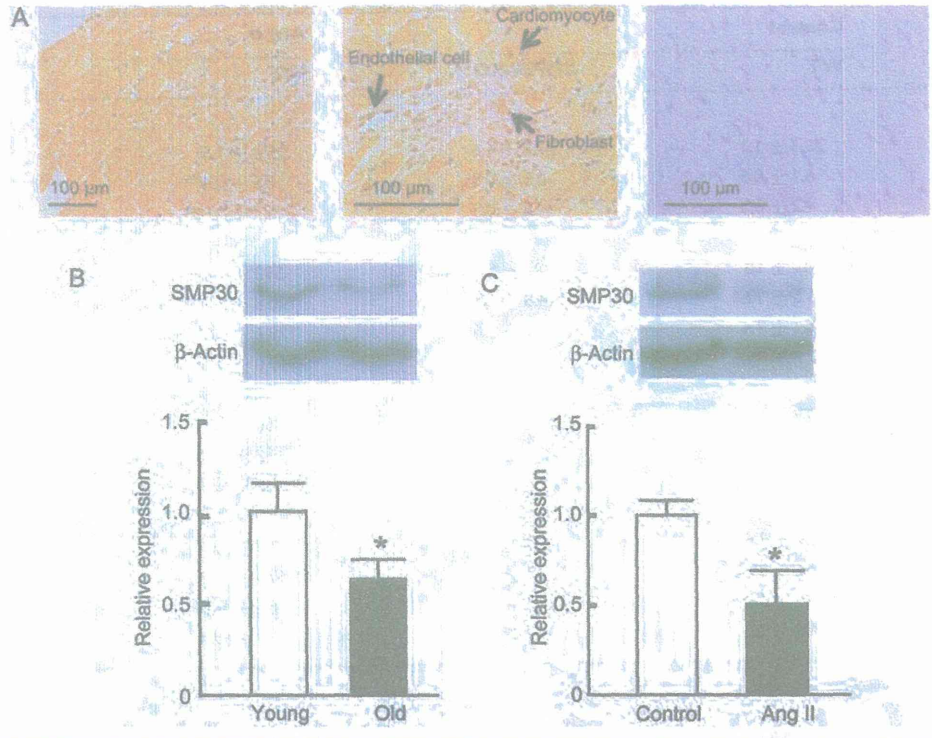

Figure 1 SMP30 expression in heart tissue. (*A*) SMP30 is expressed in cardiomyocytes, fibroblasts, and vascular endothelial cells (left, magnification ×200; middle, ×400). Right panel indicates negative control (×400). (*B*) Cardiac SMP30 expression was significantly decreased by 40% at 12-month-old WT mice (old) compared with 3-month-old WT mice (young). (*C*) Cardiac SMP30 expression was significantly decreased by 50% after Ang II infusion for 14 days in WT mice. Results are mean ± SD from 3 mice in each group. *$P < 0.05$ vs. young mice or control.

2.9 *In vivo* terminal deoxynucleotidyl transferase-mediated dUTP nick end- labellingassay

Apoptosis was detected by the terminal deoxynucleotidyl transferase-mediated dUTP nick end-labelling (TUNEL) method (CardioTACS *In Situ* Apoptosis Detection Kit, Trevigen, Inc., Gaithersburg, MD, USA) according to the manufacturer's instructions. TUNEL-positive nuclei were counted, and then expressed as a per cent of the total nuclei.[28]

2.10 Senescence-associated β-galactosidase activity

Senescence-associated β-galactosidase (SA-β-gal) staining was performed according to the manufacturer's protocol (BioVision, Inc., Mountain View, CA, USA).[29] SA-β-gal-positive cardiomyocytes were visualized as blue colour under light microscopy, and positive cells for SA-β-gal activity were counted.

2.11 Reverse transcription polymerase chain reaction

Total RNA was extracted from the snap-frozen left ventricle using TRIzol reagent (Invitrogen, Carlsbad, CA, USA).[28] Reverse transcription polymerase chain reaction (RT–PCR) was performed using the PrimeScript RT–PCR Kit (Takara Bio, Inc., Otsu, Japan) according to the manufacturer's instructions. Primers were designed on the basis of GenBank sequences (p21, NM_001111099 and β-actin, NM_007393). The optical density of the bands was quantified using the NIH imageJ software.

2.12 Statistical analysis

All data were expressed as mean ± SD. Comparisons of vitamin C levels at basal conditions between WT mice and SMP30-KO mice were performed by an unpaired *t*-test. All other parameters were evaluated by two-way analysis of variance followed by multiple comparisons with the Bonferroni test using SPSS Statistics 17.0 (SPSS Japan, Inc., Tokyo, Japan). A probability value < 0.05 was considered statistically significant.

3. Results

3.1 Vitamin C levels of the heart tissue in WT mice and SMP30-KO mice

First, we measured vitamin C levels of the heart tissue in basal conditions. To avoid vitamin C deficiency, drinking water containing sufficient vitamin C was supplied for SMP30-KO mice because SMP30-KO mice were unable to synthesize vitamin C due to the lack of gluconolactonase.[10] The tissue concentrations of the vitamin C level were not significantly different between WT mice and SMP30-KO mice (45.7 ± 7.0 vs. 44.5 ± 10.2 μg/g tissue).

3.2 SMP30 expression in the heart tissue

Immunostaining revealed that SMP30 was expressed in cardiomyocytes, fibroblasts, and vascular endothelial cells in WT mice on the basis of cellular morphological characteristics (*Figure 1A*).[30] We confirmed the decrease in SMP30 expression with ageing in the WT mouse heart as